Intensity- and time-dependent anticancer effects of alternating electric fields in non-small cell lung cancer cell lines

JINJU HEO[1] and MYONGGEUN YOON[1,2]

[1]Department of Bio-medical Engineering, Korea University, Seoul 02841, Republic of Korea;
[2]Research and Development Center, FieldCure Ltd., Seoul 02852, Republic of Korea

Received December 2, 2025; Accepted February 27, 2026

DOI: 10.3892/ol.2026.15593

Abstract. Alternating electric fields (AEF), also known as tumor treating fields (TTFields), have emerged as a non-invasive anticancer modality; however, their clinical benefit in non-small cell lung cancer (NSCLC) still depends heavily on prolonged daily wear time, which often limits patient adherence due to discomfort and skin irritation. Despite recent Food and Drug Administration approval of TTFields for metastatic NSCLC, the relative contributions of field intensity and exposure duration, particularly from a quantitative and dosimetric perspective, have not been systematically evaluated. In the present study, H460 and A549 NSCLC cell lines were exposed to three TTFields regimens combining different intensity-duration configurations (0.4 V/cm for 24 h, 0.8 V/cm for 6 h and 1.6 V/cm for 3 h), and short-(48 h) and long-term (7-day) responses were assessed. TTFields significantly reduced cell viability, clonogenic survival and migratory capacity while increasing apoptotic susceptibility. Notably, treatment conditions with different intensity-duration combinations produced partially overlapping inhibitory effects, suggesting that overall exposure may contribute to the observed responses. These findings indicated that NSCLC cells respond to TTFields in a dosimetry-dependent manner and support the existence of an intensity-duration trade-off. The present study provided preliminary evidence for flexible TTFields exposure strategies while underscoring the need for energy-matched and *in vivo* validation in future research to refine treatment scheduling in NSCLC.

Correspondence to: Professor Myonggeun Yoon, Department of Bio-medical Engineering, Korea University, 145 Anam-ro, Seongbuk-gu, Seoul 02841, Republic of Korea
E-mail: radioyoon@korea.ac.kr

Key words: alternating electric fields, tumor treating fields, non-small cell lung cancer, apoptosis, treatment scheduling, clonogenic survival, cell migration

Introduction

Non-small cell lung cancer (NSCLC) accounts for 85-87% of all lung cancer cases and recent studies indicated that 30-50% of patients present with distant metastases at the time of diagnosis (1,2). Although immune checkpoint inhibitors and targeted therapies have extended survival in selected patient groups, long-term treatment efficacy remains limited by the emergence of drug resistance, immune escape and tumor heterogeneity (3). In advanced or metastatic NSCLC, conventional drug-based regimens often fail to achieve sufficient responses, underscoring the need for non-pharmacological, non-invasive therapeutic strategies that can complement existing modalities.

Against this background, alternating electric fields (AEF), commonly referred to as tumor treating fields (TTFields), have gained increasing attention (4). TTFields deliver low-intensity AEF within the 100-300 kHz range to tumor tissues, selectively targeting dividing cells. By disrupting microtubule polymerization, impairing mitotic spindle assembly and increasing dielectrophoretic forces on intracellular organelles, TTFields induce mitotic catastrophe and apoptosis in actively proliferating tumor cells (5). Since the mechanism of action is physical rather than molecular, TTFields are not affected by conventional resistance mechanisms and can be combined seamlessly with existing anticancer therapies (6,7).

Clinically, TTFields have demonstrated efficacy in glioblastoma (GBM) and malignant pleural mesothelioma, leading to Food and Drug Administration (FDA) approvals in both indications (8,9). Based on the results of the LUNAR phase III trial published in 2024, Optune Lua subsequently received FDA approval in metastatic NSCLC in combination with immune checkpoint inhibitors or docetaxel following platinum-based chemotherapy (10). This notable event positions TTFields as an established therapeutic option for NSCLC and further highlights the need to understand tumor-specific electrical responses and optimize TTFields parameters for this cancer type in the future.

Previous studies have indicated that TTFields efficacy is governed by several biophysical parameters, including field intensity and exposure duration, with even small parameter variations producing non-linear amplification of mitotic disruption (11-13). In clinical practice, prolonged daily wear time (typically ~18 h per day) is required to maximize

therapeutic benefit; however, long-term use is frequently challenged by skin irritation, discomfort associated with transducer arrays and reduced patient compliance (14). These limitations have created a growing clinical interest in identifying intensity-duration combinations capable of maintaining antitumor efficacy while reducing total wear time. Nevertheless, in NSCLC, quantitative studies that systematically evaluate the interaction between field intensity and exposure duration (dose-schedule dependency) remain scarce (15). Therefore, in the present study, a multilayered profiling of both short-term (48 h) and long-term (7-day) responses to TTFields in NSCLC cell lines (H460 and A549) was performed to elucidate the relationship between field intensity, exposure duration and antitumor efficacy. This approach provides quantitative and functional insight into TTFields response patterns in NSCLC, which may potentially serve as a basis for future investigations of parameter-dependent effects.

Materials and methods

Cell culture. H460 and A549 NSCLC cell lines were obtained from the Korean Cell Line Bank (cat. nos. 30096 and 10185, respectively; Korean Cell Line Research Foundation). Cells were cultured in RPMI-1640 medium (Welgene, Inc.) supplemented with 10% fetal bovine serum and 1% penicillin-streptomycin (Thermo Fisher Scientific, Inc.). Cultures were maintained at 37˚C in a humidified 5% CO_2 incubator. For routine maintenance, cells were seeded at an initial density of $5x10^5$ cells and subcultured every 3-4 days. All experiments were performed using healthy cells in the logarithmic growth phase.

TTFields setup. AEF were generated using a custom-built system consisting of a function generator (cat. no. AFG-2112; Good Will Instrument Co., Ltd.), a high-voltage amplifier (cat. no. A303; A.A. Lab Systems Ltd.) and a sterilized parallel-plate electrode assembly. Prior to cell seeding, electrode wires were sterilized, fully air-dried and attached to culture dishes inside a biosafety cabinet. The assembled dish-wire system was then UV-sterilized for at least 30 min. Two electrodes were positioned 3 cm apart at the center of the dish to ensure uniform field distribution. A sine-wave signal at 150 kHz was used for all experiments.

Electric field measurement and verification. The applied electric field intensity (V/cm) was experimentally measured and verified to ensure accurate and reproducible field delivery. Voltage measurements were performed using an OWON HDS1022M-N digital oscilloscope (OWON Technology, Inc.) equipped with a Keysight N2791A 25 MHz differential probe (Keysight Technologies, Inc.). The probe tips were positioned at the center region between the insulated electrode wires with a fixed inter-probe distance of 1 cm, corresponding to the area where cells were cultured. The measured voltage difference was used to calculate the electric field intensity (V/cm) and measurements were repeated to confirm consistency across experimental conditions.

TTFields treatment. To assess the intensity-time dependency of TTFields, cells were exposed to one of three conditions: Protocol (P)1, 0.4 V/cm for 24 h; P2, 0.8 V/cm for 6 h; or P3, 1.6 V/cm for 3 h. These conditions represent progressively higher field intensities with proportionally shorter exposure durations. Control groups were cultured under identical conditions without electric field stimulation. All treatments were performed under carefully controlled thermal conditions. During preliminary testing, high-intensity TTFields exposure was associated with a modest temperature increase (~1˚C) under standard incubator settings. To minimize potential Joule heating effects, incubator temperature settings were adjusted such that the effective culture temperature was maintained at 37˚C across all experimental conditions. Medium temperature was monitored during electric field exposure using a non-contact infrared thermometer (FLUKE 62 MAX; Fluke Corporation), which was employed to avoid physical disturbance of the culture environment and interference with the electric field setup. For detailed temperature monitoring experiments presented in Fig. S1, temperature was recorded at 30-min intervals over a 3-h period using a contact-type data logger thermometer (model TES-1384; TES Electrical Electronic Corp.). The temperature probe was fixed at the center of the culture dish and positioned ~1.5 cm away from the electrode surface. Representative temperature profiles before and after thermal compensation are provided in Fig. S1.

Cell imaging. At 48 h after TTFields exposure, overall cell density and cluster formation patterns were examined using an inverted phase-contrast microscope (ECLIPSE TS100; Nikon Corporation) equipped with a digital camera (IMTcam3; i-Solution, Inc.). Representative images were captured to document qualitative morphological differences across treatment groups.

Cell viability assessment. At 48 h after TTFields exposure, cells were harvested using trypsin-EDTA and viable cell numbers were determined by trypan blue exclusion. Equal numbers of viable cells from each group were re-seeded into 96-well plates (500-1,000 cells per well) and allowed to attach overnight. The following day, the medium was replaced with fresh medium containing WST-8 reagent (Quanti-MAX™ WST-8 Cell Viability Assay Kit; cat. no. QM2500; Biomax) and plates were incubated for 1 h at 37˚C. Absorbance at 450 nm was measured using a microplate reader (PHOmo; Autobio Labtec Instruments). For direct viability assessment, a portion of harvested cells was stained with trypan blue and counted manually using a hemocytometer (DHC-N01-5; INCYTO). All experiments were performed in triplicate.

Colony formation assay. After TTFields exposure, cells were harvested and seeded into 6-well plates at low density (500-1,000 cells per well). Cells were cultured in complete medium without soft agar and maintained for 10-14 days at 37˚C in a humidified incubator with 5% CO_2, with the medium replaced every 3-4 days. Colonies were washed with phosphate-buffered saline (PBS), fixed with 100% methanol for 15 min at room temperature (20-25˚C) and stained with 0.5% crystal violet for 20 min at room temperature. Plates were then rinsed with distilled water and air-dried. After drying, colonies containing ≥50 cells were counted by visual inspection of

the entire well surface. Survival fraction=(colonies in treated group)/(colonies in control group). All experiments were conducted in triplicate.

Migration assay. Cell migration was evaluated using Transwell chambers (8-μm pore size; Corning, Inc.). After TTFields treatment, 4,000 cells in 200 μl of serum-free medium were seeded into the upper chamber and complete medium containing 10% fetal bovine serum (FBS; Gibco; Thermo Fisher Scientific, Inc.) was added to the lower chamber as a chemoattractant. Cells were incubated for 18-24 h at 37˚C in a humidified incubator with 5% CO_2. Following incubation, the upper chamber medium was removed by gentle pipetting and non-migrated cells on the upper membrane surface were carefully removed with PBS. Migrated cells on the lower surface were fixed with 100% methanol for 10-15 min at room temperature and stained with 0.5% crystal violet for 20 min at room temperature. Representative images of stained membranes were captured using a light microscope. All experiments were performed in triplicate.

Apoptosis analysis by Annexin V/propidium iodide (PI) staining. Apoptosis was assessed using an Annexin V-FITC Apoptosis Detection Kit (BioVision, Inc.). H460 and A549 cells were treated under the indicated experimental conditions. After treatment, cells were harvested, washed twice with cold PBS and resuspended in 1X binding buffer (provided in the kit). Cells were stained with Annexin V-FITC and PI according to the manufacturer's instructions and incubated for 15 min at room temperature in the dark. The staining mixture contained 5 μl Annexin V-FITC and 5 μl PI per 100-μl cell suspension. Flow cytometric analysis was performed using a BD FACSAria™ flow cytometer (BD Biosciences). At least 10,000 events per sample were acquired. Annexin V-FITC and PI fluorescence signals were detected using a 488 nm excitation laser and appropriate emission filters. Apoptotic cell populations were classified as viable cells (Annexin V^-/PI^-), early apoptotic cells (Annexin V^+/PI^-), late apoptotic or secondary necrotic cells (Annexin V^+/PI^+), and necrotic cells (Annexin V^-/PI^+). The percentage of total apoptotic cells, defined as the sum of early and late apoptotic populations, was calculated for quantitative analysis. Data were analyzed using FlowJo software (version 10; BD Biosciences).

Western blotting analysis. Cells were collected after TTFields exposure and washed with cold PBS. Total protein was extracted using RIPA buffer (Thermo Fisher Scientific, Inc.) containing protease and phosphatase inhibitors, incubated on ice and centrifuged at 12,000 x g for 15 min at 4˚C. Protein concentrations were determined using a BCA assay. Equal amounts of protein (20-30 μg) were denatured at 95˚C for 5 min and separated on 12% SDS-polyacrylamide gels, followed by transfer onto PVDF membranes. Membranes were blocked with 5% BSA in TBST (0.1% Tween-20) for 1 h at room temperature and incubated overnight at 4˚C with primary antibodies against poly (ADP-ribose) polymerase (PARP; cat. no. 9542; Cell Signaling Technology, Inc.) and β-actin (cat. no. 3700; Cell Signaling Technology, Inc.) (both diluted 1:1,000). After washing, membranes were incubated with HRP-conjugated secondary antibodies (cat. nos. rabbit IgG #7074; mouse IgG #7076; Cell Signaling Technology, Inc.; diluted 1:1,000) for 1 h at room temperature. PARP was detected using Atto Ultimate Sensitivity ECL (cat. no. 34579; Thermo Fisher Inc.) and β-actin was detected using standard ECL. Images were acquired using an iBright CL750 imaging system (Thermo Fisher Scientific, Inc.).

Statistical analysis. Statistical analyses were performed using GraphPad Prism software (version 8.0; Dotmatics). For comparisons between two groups, an unpaired two-tailed Student's t-test was used. For comparisons involving more than two experimental groups, one-way analysis of variance was applied, followed by Tukey's multiple comparisons post hoc test to account for familywise error rate inflation. Data are presented as mean ± standard deviation from at least three independent experiments. $P<0.05$ was considered to indicate a statistically significant difference.

Results

TTFields disrupt early morphology and reduce short-term cell viability in NSCLC cells. Phase-contrast imaging performed after 2 days of treatment revealed clear intensity-dependent morphological alterations in both H460 and A549 cells following TTFields exposure. Compared with untreated controls, TTFields-treated cells exhibited reduced monolayer confluence (Fig. 1A). These disruptions were most apparent at 0.8 and 1.6 V/cm, where sparsely populated regions and diminished cellular clustering were prominent. Consistent with these morphological changes, direct cell counting at the 2-day experimental endpoint demonstrated a proportional reduction in viable cell numbers across all TTFields conditions (Fig. 1B). Both H460 and A549 demonstrated significantly decreased viability at endpoint, with the most notable reduction observed at 1.6 V/cm, indicating a progressively stronger inhibitory effect with increasing field intensity.

TTFields reduce long-term clonogenic survival, with similar inhibitory effects at 0.4 and 0.8 V/cm. Colony formation assays revealed that TTFields markedly impaired the clonogenic capacity of both H460 and A549 cells (Fig. 2A). Compared with untreated controls, all TTFields-treated groups exhibited reduced colony numbers and smaller colony clusters. Notably, 0.4 and 0.8 V/cm conditions produced similar levels of inhibition, indicating a similar extent of colony reduction and diminished cluster formation. By contrast, 1.6 V/cm resulted in the most notable suppression, with sparse or nearly absent colonies in both cell lines. Survival fraction analysis performed in three independent experiments consistently demonstrated this trend, indicating a plateau in inhibitory effect between 0.4 and 0.8 V/cm, followed by a significant decline at 1.6 V/cm (Fig. 2B).

Long-term TTFields exposure induces mild inhibition under P1 and 2 and marked suppression under P3. To evaluate sustained TTFields effects, cells were cultured for 7 days under three stimulation protocols (P1-3), each representing distinct intensity-duration combinations (Fig. 3A). Cell counting on day 7 revealed that both P1 and 2 produced mild reductions in total cell number, whereas P3 led to a significant

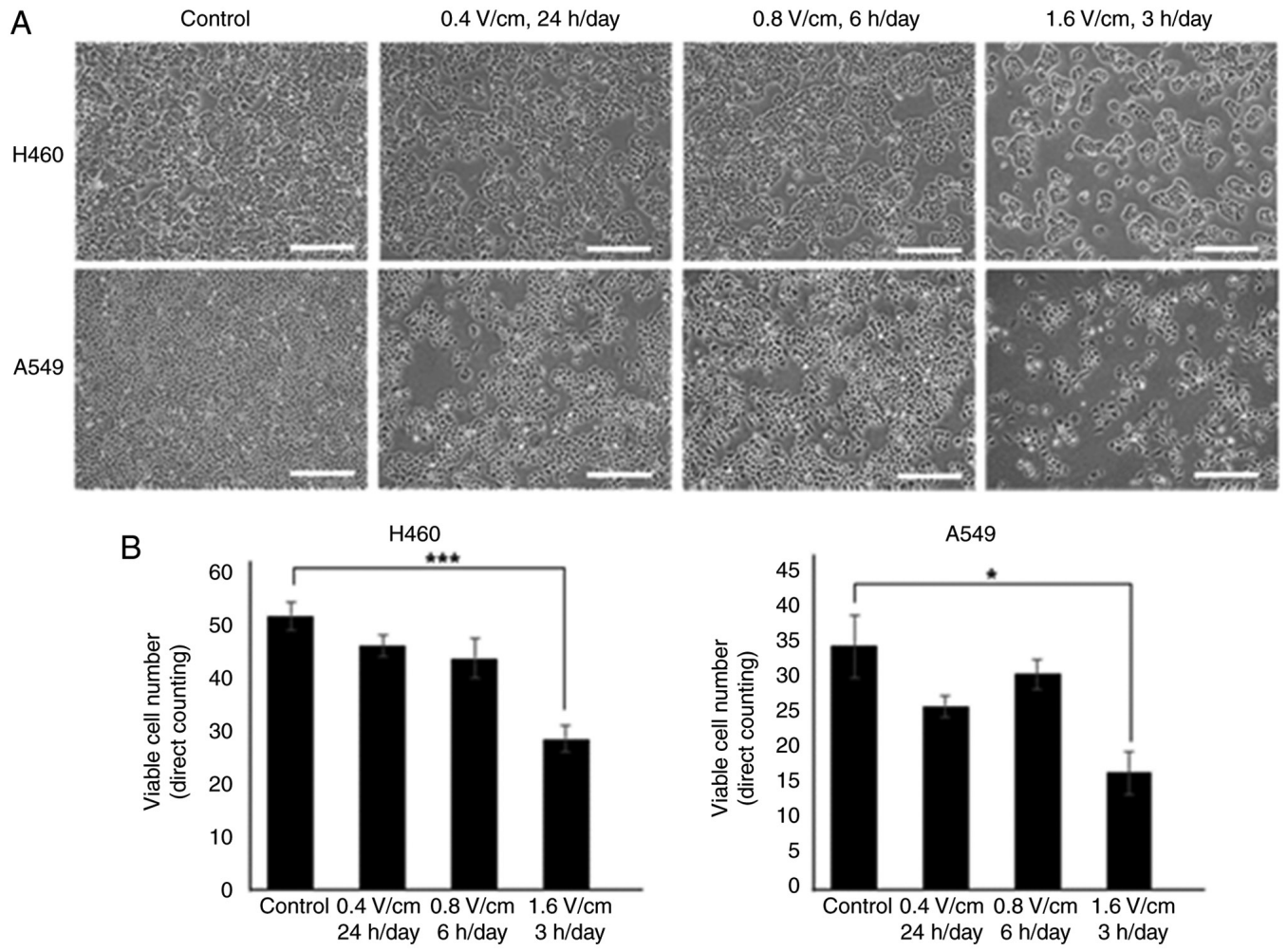

Figure 1. Early morphological alterations and reduced cell viability in H460 and A549 cells following TTFields exposure. (A) Representative phase-contrast images acquired at the 48 h endpoint (maximum active exposure of 24 h/day) illustrate relative changes in monolayer confluence, cellular morphology and adherence following TTFields treatment. These images are presented to highlight qualitative differences among conditions and are not intended to reflect absolute cell numbers. (B) Quantitative analysis of viable cell numbers at the 48 h endpoint was performed by direct cell counting across multiple independent fields and experiments. The analysis demonstrates a reduction in cell number under TTFields exposure, with the strongest inhibitory effect observed at 1.6 V/cm. Scale bar, 250 μm. Data are presented as mean ± SD. *P<0.05 and ***P<0.001. TTFields, tumor treating fields.

decrease, leaving only a small population of surviving cells (Fig. 3B). This indicates that long-term cytoreduction becomes notable only under the strongest stimulation condition. WST-8 analysis supported these observations (Fig. 3C). Metabolic activity exhibited a modest decline under P1, followed by a stronger reduction under P2 and the lowest activity under P3. These findings demonstrated differential inhibitory patterns across the three stimulation protocols, with mild long-term suppression under P1 and 2 and a marked loss of proliferative capacity under the P3 protocol.

TTFields induce differential apoptosis-associated signaling and migration responses across intensity-duration conditions. Western blotting analysis revealed that cleaved PARP was detectable at low levels in control cells, likely reflecting basal stress associated with culture conditions (Fig. 4A). When normalized to total PARP, the cleaved PARP/total PARP ratio exhibited no marked change under lower intensity-duration conditions (P1 and 2), whereas a marked increase was observed under the highest condition (P3), indicating a threshold-dependent enhancement of PARP cleavage. This effect was more evident in H460 cells compared with that in A549 cells, suggesting cell-line-specific differences in apoptotic sensitivity. By contrast, Annexin V/PI staining (Fig. 4B) revealed a more gradual apoptotic response, in which P1 induced only minimal changes, P2 increased early apoptosis and P3 produced the highest levels of both early and late apoptotic cells. Consistent with these trends, Transwell migration analysis (Fig. 4C) revealed that P1 and 2 were associated with only mild reductions in cell motility, whereas P3 was associated with a more notable decrease in migration in both H460 and A549 cells.

Discussion

TTFields have been extensively investigated in GBM, whereas research in lung cancer remains comparatively limited (9). Since NSCLC exhibits biological behaviors and treatment responses that differ markedly from those of GBM, stimulation parameters optimized for GBM cannot be assumed to translate directly to NSCLC (16,17). Nonetheless, majority of NSCLC studies have adopted GBM-derived settings despite marked

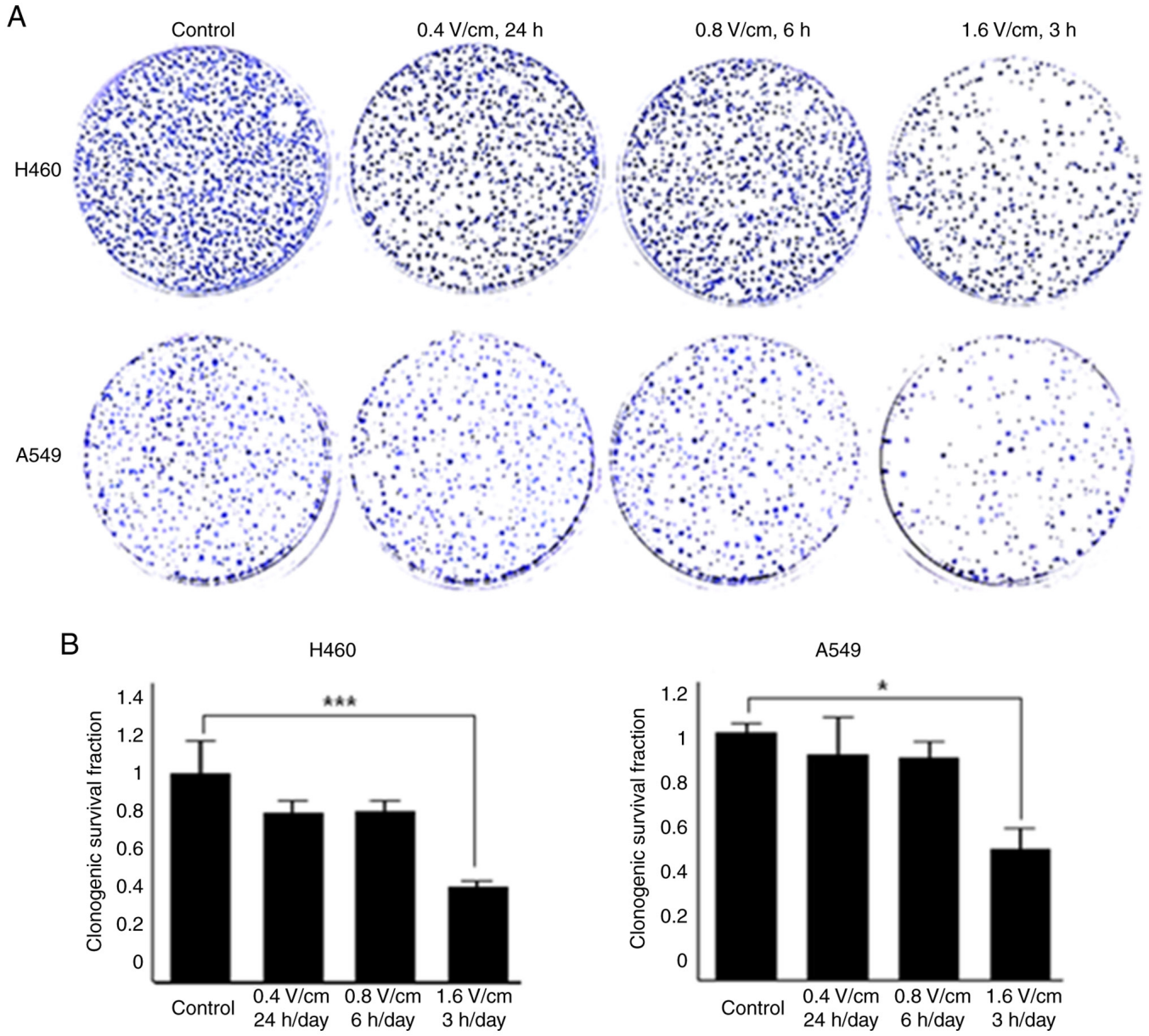

Figure 2. Effects of TTFields on clonogenic growth in non-small cell lung cancer cell lines. (A) Representative colony formation images of H460 and A549 cells following TTFields exposure. Both cell lines exhibited reduced colony number and colony size compared with untreated controls. The 0.4 and 0.8 V/cm groups exhibited similar inhibitory patterns, whereas 1.6 V/cm resulted in the strongest suppression, with markedly fewer surviving colonies. (B) Quantitative analysis of clonogenic survival fraction calculated from colony formation assays. Data are presented as mean ± SD from three independent experiments. *P<0.05 and ***P<0.001. TTFields, tumor treating fields.

biophysical differences between the two tumor types (18,19), underscoring the need to evaluate NSCLC-specific responses. In the present study, two NSCLC cell lines across a range of short-term and long-term exposure schedules were examined to explore their responsiveness to AEF delivered at different intensities. This experimental framework was designed to assess how NSCLC cells integrate field intensity and exposure duration, providing a structured basis in interpreting their combined influence on cellular responses.

Notably, these findings hold practical relevance for clinical translation. Current treatment protocols emphasize prolonged daily exposure, typically ~18 h, to maximize therapeutic efficacy (20). However, extended wear time often leads to skin irritation, discomfort associated with transducer arrays and notable restrictions in daily activities, ultimately compromising patient adherence (21-23). Within this clinical context, the present study observations indicated that similar inhibitory effects can be achieved through alternative combinations of field intensity and exposure duration, rather than through prolonged stimulation alone. This finding is consistent with the concept of an intensity-duration trade-off and aligns with growing interest in parameter configurations that may improve treatment tolerability while maintaining antitumor activity (24-28). However, these implications should be viewed as preliminary and interpreted with appropriate caution.

A key consideration is that the interpretation of TTFields efficacy should account for the physical and dosimetric principles governing energy deposition within conductive biological media. Since the power density dissipated by an alternating electric field scales with the square of the field intensity ($P \propto$

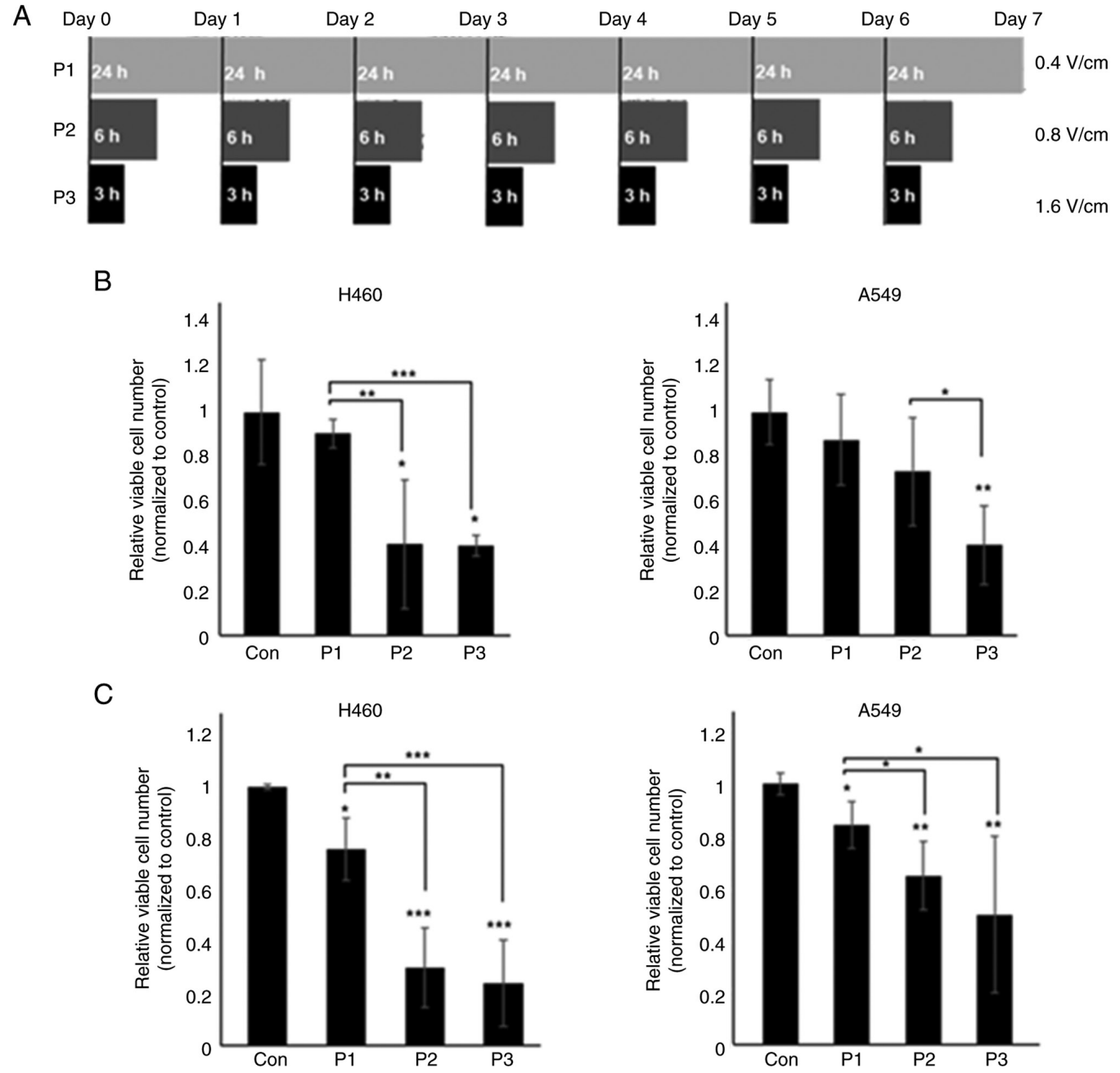

Figure 3. Long-term inhibitory effects of TTFields under three stimulation protocols. (A) Schematic representation of the three TTFields protocols (P1-3), each corresponding to a distinct intensity-duration combination. (B) Total cell counts after 7 days of culture demonstrating mild inhibition under P1 and 2, and a marked reduction in surviving cells under P3. (C) WST-8 metabolic activity demonstrates a mild decrease under P1, with significantly stronger suppression under P2 and 3. Data are presented as mean ± SD from three independent experiments. *P<0.05, **P<0.01 and ***P<0.001. Con, control; TTFields, tumor treating fields; P1, 0.4 V/cm for 24 h; P2, 0.8 V/cm for 6 h; P3, 1.6 V/cm for 3 h.

σE^2), the time-integrated power density and thus, total delivered energy, can be expressed as a function of field intensity and exposure duration ($\propto \sigma E^2 t$) (29). Within this framework, treatment regimens that differ in intensity and duration are not necessarily energy-equated, yet biological responses may converge within certain effective dose ranges. In the present study, the similar biological responses observed under the 0.4 V/cm for 24 h and 0.8 V/cm for 6 h conditions are consistent with the notion that partially overlapping ranges of effective energy exposure can produce similar levels of growth inhibition, even when regimens are not strictly energy-matched. By contrast, the enhanced cytotoxic effects observed under the highest-intensity condition (1.6 V/cm for 3 h) are more parsimoniously explained by increased total energy delivery, although the contribution of intensity-dependent biological thresholds cannot be fully excluded. Taken together, and in line with previous studies describing diminishing returns with prolonged exposure, these observations underscored that TTFields efficacy is best interpreted within an integrated dosimetric framework reflecting combined interactions between intensity and duration, rather than dominance of individual parameters in isolation (30-32).

From a biological and therapeutic perspective, these dosimetric considerations also warrant cautious interpretation

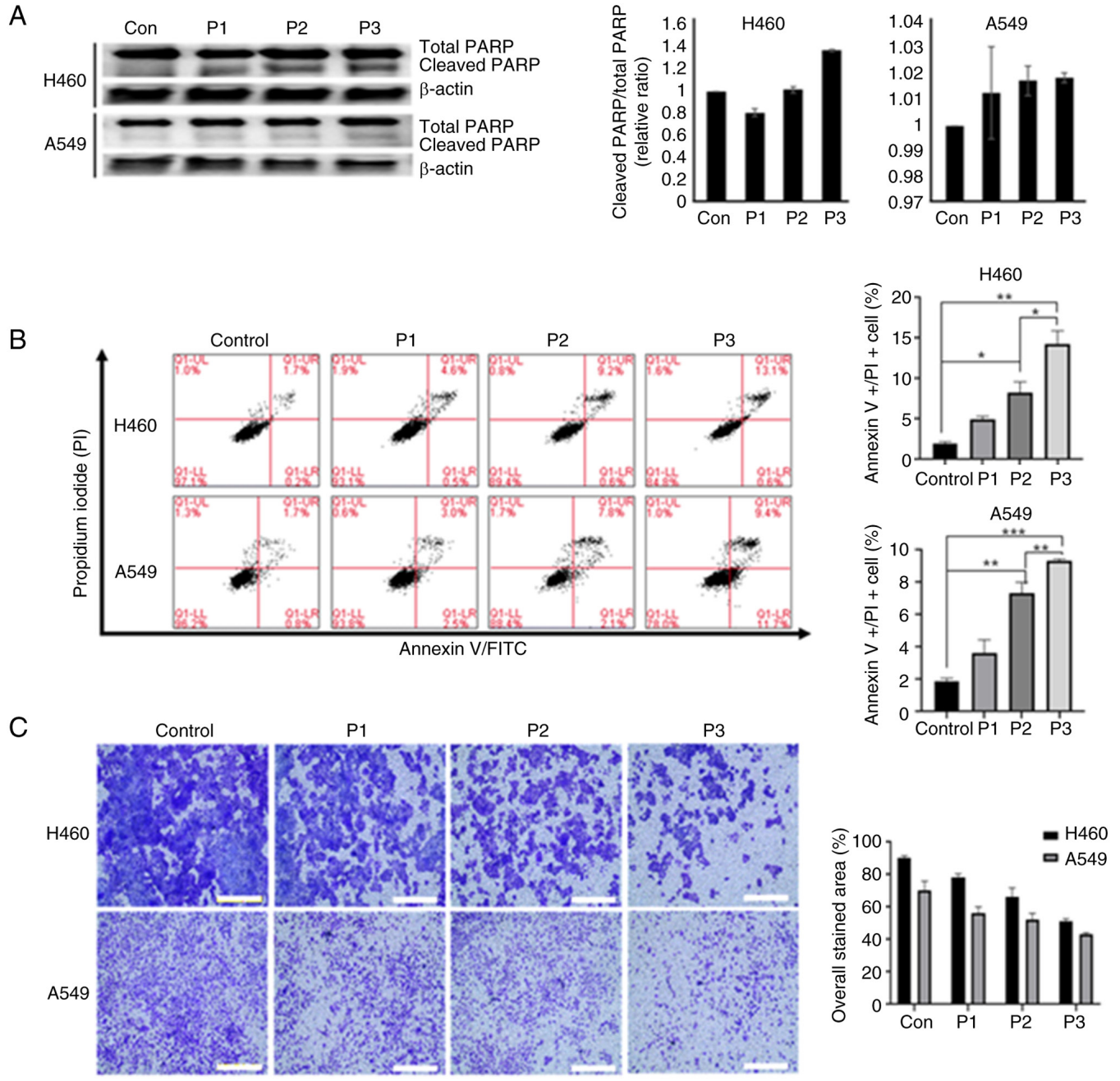

Figure 4. Effects of long-term TTFields exposure on apoptosis-associated signaling and migration in non-small cell lung cancer cells. (A) Western blotting analysis of total PARP and cleaved PARP in H460 and A549 cells after long-term TTFields exposure. The ratio of cleaved PARP to total PARP was quantified by densitometric analysis and is presented as a bar graph. (B) Annexin V/PI flow cytometry demonstrating a progressive increase in apoptotic populations, with P3 exhibiting the highest levels of early and late apoptosis. (C) Transwell migration assay revealing migration of H460 and A549 cells under different TTFields intensity-duration conditions. Representative crystal violet-stained images and quantification of overall stained area are presented for control, P1, 2 and 3. Scale bar, 250 μm. *P<0.05, **P<0.01 and ***P<0.001. Con, control; TTFields, tumor treating fields; PARP, poly (ADP-ribose) polymerase; PI, propidium iodide; P1, 0.4 V/cm for 24 h; P2, 0.8 V/cm for 6 h; P3, 1.6 V/cm for 3 h.

of high-intensity, short-duration TTFields regimens. Abbreviated exposure windows may permit tumor cell repopulation during off-treatment intervals and could limit synergistic interactions with cell-cycle-dependent therapies, such as chemotherapy, which are known to benefit from prolonged or continuous TTFields exposure (33,34). Accordingly, modulation of field intensity should be considered within a broader therapeutic context that accounts for treatment scheduling and combination strategies, rather than as a standalone optimization approach.

Lastly, the present study has inherent limitations associated with its *in vitro* experimental design. The simplified culture system does not capture the complexity of the tumor microenvironment, including tissue architecture, stromal interactions and immune components that may influence electric field distribution and treatment response *in vivo*. Furthermore, the electric-field geometry applied here differs from clinical conditions and the mechanistic pathways underlying dosimetry-dependent TTFields responses were only partially explored. Future studies incorporating *in vivo* tumor

models, detailed electric field and thermal simulations and expanded molecular analyses will therefore be key to validate the biological relevance and translational feasibility of alternative intensity-duration configurations.

Acknowledgements

Not applicable.

Funding

The present study was supported by National Research Foundation of Korea (NRF) grants funded by the Korean government (MSIT; grant nos. NRF-2021R1A2C2008695 and NRF-2022R1A2C1010337). The present study was also supported by a Korea Medical Device Development Fund grant funded by the Korean Government (the Ministry of Science and ICT, the Ministry of Trade, Industry and Energy, the Ministry of Health & Welfare and the Ministry of Food and Drug Safety; grant nos. 1711196423 and RS-2023-00254868).

Availability of data and materials

The data generated in the present study may be requested from the corresponding author.

Authors' contributions

JH conceived and performed the present study, carried out all experiments, analyzed the data and wrote the manuscript. MY contributed to the conception and interpretation of the study, provided supervision and critically revised the manuscript. JH and MY confirm the authenticity of all the raw data. Both authors have read and approved the final manuscript.

Ethics approval and consent to participate

Not applicable.

Patient consent for publication

Not applicable.

Competing interests

The authors declare that they have no competing interests.

References

1. Huang Q, Li Y, Huang Y, Wu J, Bao W, Xue C, Li X, Dong S, Dong Z and Hu S: Advances in molecular pathology and therapy of non-small cell lung cancer. Signal Transduct Target Ther 10: 186, 2025.
2. Ni L, Liu Z, Xiang L, Li Y and Zhang Y: Comprehensive evaluation of risk factors for LNM and distant metastasis in patients with NSCLC. Sci Rep 15: 30809, 2025.
3. Sandhbor P, John G, Bhat S and Goda JS: Immune response recalibration using immune therapy and biomimetic nano-therapy against high-grade gliomas and brain metastases. Asian J Pharm Sci 20: 101021, 2025.
4. Shams S and Patel CB: Anti-cancer mechanisms of action of therapeutic alternating electric fields [tumor treating fields (TTFields)]. J Mol Cell Biol 14: mjac047, 2022.
5. American Cancer Society: Treating non-small cell lung cancer. Available at: https://www.cancer.org/cancer/types/lung-cancer/treating-non-small-cell.html Accessed: November 29, 2025.
6. Yu A, Zeng J, Yu J, Cao S and Li A: Theory and application of TTFields in newly diagnosed glioblastoma. CNS Neurosci Ther 30: e14563, 2024.
7. Lin W, Wang Y, Li M, Feng J, Yue Y, Yu J, Hu Y and Suo Y: Tumor treating fields enhance anti-PD therapy by improving CCL2/8 and CXCL9/CXCL10 expression through inducing immunogenic cell death in NSCLC models. BMC Cancer 25: 489, 2025.
8. Ballo MT, Conlon P, Lavy-Shahaf G, Kinzel A, Vymazal J and Rulseh AM: Association of Tumor Treating Fields (TTFields) therapy with survival in newly diagnosed glioblastoma: A systematic review and meta-analysis. J Neurooncol 164: 1-9, 2023.
9. Ceresoli GL and Gianoncelli L: Tumor treating fields (TTFields) therapy in unresectable pleural mesothelioma: Overview of efficacy, safety, and future outlook. Curr Treat Options Oncol 26: 398-414, 2025.
10. Leal T, Kotecha R, Ramlau R, Zhang L, Milanowski J, Cobo M, Roubec J, Petruzelka L, Havel L, Kalmadi S, *et al*: Tumor treating fields therapy with standard systemic therapy versus standard systemic therapy alone in metastatic non-small-cell lung cancer following progression on or after platinum-based therapy (LUNAR): A randomised, open-label, pivotal phase 3 study. Lancet Oncol 24: 1002-1017, 2023.
11. Tanzhu G, Chen L, Xiao G, Shi W, Peng H, Chen D and Zhou R: The schemes, mechanisms and molecular pathway changes of tumor treating fields (TTFields) alone or in combination with radiotherapy and chemotherapy. Cell Death Discov 8: 416, 2022.
12. Liu M, Su Z, Hagemann PP, Fischer M and Linnebacher M: Optimization of tumor treating fields (TTFields) frequency and treatment duration in colorectal cancer cells. Cancer Med 14: e70976, 2025.
13. Oh G, Jo Y, Gi Y, Hong J, Kim J, Lee B and Yoon M: Correlation between impulse magnitude and inhibition of cell proliferation in alternating electric fields therapy. AIP Adv 13: 085005, 2023.
14. Zang M, Zhu S and Niu Q: Advancement in tumor treating fields of mechanism, clinical applications, and future directions. Discov Oncol 16: 1049, 2025.
15. Wainer-Katsir K, Haber A, Fishman H, Ding L, Story MD, Du R, Kahlert UD, Mannarino L, Mirimao F, Lupi M, *et al*: The transcriptomic fingerprint of cancer response to tumor treating fields (TTFields). Cell Death Discov 11: 319, 2025.
16. Kutuk T, Atak E, La Rosa A, Kotecha R, Mehta MP and Chuong MD: Tumor treating fields: Narrative review of a promising treatment modality for cancer. Chin Clin Oncol 12: 64, 2023.
17. Urman N, Nave A and Bozmos B: P25.10 Computational simulations on safety of tumor treating fields delivered to the lungs in mesothelioma and NSCLC. J Thorac Oncol 16 (Suppl): S386, 2021.
18. Yue Y, Wang Y, Feng J, Yao M and Suo Y: Tumor treating fields suppress tumor cell growth and induce immunogenic cell death biomarkers in biliary tract cancer cell lines. Sci Rep 15: 30611, 2025.
19. Berkelmann L, Bader A, Meshksar S, Dierks A, Hatipoglu Majernik G, Krauss JK, Schwabe K, Manteuffel D and Ngezahayo A: Tumour-treating fields (TTFields): Investigations on the mechanism of action by electromagnetic exposure of cells in telophase/cytokinesis. Sci Rep 9: 7362, 2019.
20. Gates TJ, Zbidat S, Deniz K, Padmanabhan S, Ladner K, Sarkari A, Zhao X, Davidi S, Blatt R, Cahal S, *et al*: Protocol for applying tumor treating fields in mouse models of cancer using the inovivo system. STAR Protoc 6: 103535, 2025.
21. Lacouture ME, Anadkat MJ, Ballo MT, Iwamoto F, Jeyapalan SA, La Rocca RV, Schwartz M, Serventi JN and Glas M: Prevention and management of dermatologic adverse events associated with tumor treating fields in patients with glioblastoma. Front Oncol 10: 1045, 2020.
22. Mrugala MM, Shi W, Iwomoto F, Lukas RV, Palmer JD, Suh JH and Glas M: Global post-marketing safety surveillance of tumor treating fields (TTFields) therapy in over 25,000 patients with CNS malignancies treated between 2011-2022. J Neurooncol 169: 25-38, 2024.
23. Chen X, Zhang Y, Zhao Q, Bai L, Chen X and Zhou Z: Management of dermatologic adverse events associated with tumor treating fields in patients with glioblastoma multiforme: A 27-case series. Asia Pac J Oncol Nurs 9: 100095, 2022.

24. Mahgoub E, Hussain A, Sharifi M, Falahati M, Marei HE and Hasan A: The therapeutic effects of tumor treating fields on cancer and noncancerous cells. Arab J Chem 14: 202110, 2021.
25. Gatson NTN, Ornelas S, Manikowski J, Toms SA and Leese E: Tumor treating fields (TTFields) therapy skin safety and prevention strategy using a fractionated schema protocol (3-days on/1-day off), effect on skin adverse events. J Clin Oncol 41 (16 Suppl): e14030, 2023.
26. Li X, Liu K, Xing L and Rubinsky B: A review of tumor treating fields (TTFields): Advancements in clinical applications and mechanistic insights. Radiol Oncol 57: 279-291, 2023.
27. Khagi S, Kotecha R, Gatson NTN, Jeyapalan S, Abdullah HI, Avgeropoulos NG, Batzianouli ET, Giladi M, Lustgarten L and Goldlust SA: Recent advances in tumor treating fields (TTFields) therapy for glioblastoma. Oncologist 30: oyae227, 2025.
28. Szklener K, Bilski M, Nieoczym K, Mańdziuk D and Mańdziuk S: Enhancing glioblastoma treatment through the integration of tumor-treating fields. Front Oncol 13: 1274587, 2023.
29. Mikic N, Gentilal N, Cao F, Lok E, Wong ET, Ballo M, Glas M, Miranda PC, Thielscher A and Korshoej AR: Tumor-treating fields dosimetry in glioblastoma: Insights into treatment planning, optimization, and dose-response relationships. Neurooncol Adv 6: vdae032, 2024.
30. Korshoej AR: Estimation of TTFields intensity and anisotropy with singular value decomposition: A new and comprehensive method for dosimetry of TTFields. In: Makarov S, Horner M and Noetscher G (eds). Brain and Human Body Modeling: Computational Human Modeling at EMBC 2018. Cham (CH): Springer, pp173-193, 2019.
31. Bomzon Z, Wenger C, Proescholdt M and Mohan S: Tumor-treating fields at EMBC 2019: A roadmap to developing a framework for TTFields dosimetry and treatment planning. In: Makarov SN, Noetscher GM and Nummenmaa A (eds). Brain and Human Body Modeling 2020: Computational Human Models Presented at EMBC 2019 and the BRAIN Initiative® 2019 Meeting. Cham (CH): Springer, pp3-17, 2021.
32. Jo Y, Sung J, Jeong H, Hong S, Jeong YK, Kim EH and Yoon M: Effectiveness of a fractionated therapy scheme in tumor treating fields therapy. Technol Cancer Res Treat 18: 1533033819845008, 2019.
33. Koltun B, Voloshin T, David C, Kan T, Barsheshet Y, Volodin A, Cahal S, Tempel-Brami C, Shai M, Jacobovitch S, *et al*: Cancer cell permeability induced by tumor treating fields (TTFields) as a physical approach to improve chemotherapy uptake and overcome multidrug resistance. Mol Cancer Ther 24: 1815-1825, 2025.
34. Amodeo R, Morosi L, Meroni M, Bello E, Timo S, Frapolli R, D'Incalci M and Lupi M: Tumor treating fields enhance chemotherapy efficacy by increasing cellular drug uptake and retention in mesothelioma cells. Am J Cancer Res 15: 271-285, 2025.